JMEPEG (2015) 24:2665–2669
DOI: 10.1007/s11665-015-1553-7

1059-9495/$19.00

Microstructure and Mechanical Properties of Granular Pearlite Steel After Equal Channel Angular Pressing

Yi Xiong, Tiantian He, Pengyan Li, Lufei Chen, Fengzhang Ren, and Alex A. Volinsky

(Submitted September 9, 2014; in revised form April 10, 2015; published online May 19, 2015)

Equal channel angular pressing (ECAP) of granular pearlite high carbon steel was carried out at room temperature via the Bc route. The microstructure evolution was investigated by means of scanning and transmission electron microscopy, and the mechanical properties of granular pearlite steel were measured by tensile and microhardness testing. After four passes, the microstructure was obviously refined. An ultrafine microduplex structure with 400 nm equiaxed ferrite grains and 200 nm cementite particles were formed. The yield strength, ultimate tensile strength, microhardness, and the ratio of the yield to tensile strength increased with the number of ECAP passes, however, the elongation slightly reduced. The tensile fracture morphology changes gradually from ductile fracture to ductile and quasi-cleavage mixed fracture.

Keywords ECAP, granular pearlite, mechanical properties, microstructure

1. Introduction

Due to the high strength, hardness, and good wear-ability, high carbon steel is widely used in tools and dies. However, poor toughness and ductility limit its industrial applications. Thus, it is important to extend the use of high carbon steel to industrial applications. Grain refinement can simultaneously enhance material strength and toughness. There are many techniques of grain refinement for high carbon steels associated with equal channel angular pressing (ECAP) (Ref 1), high pressure torsion (Ref 2, 3), ball milling (Ref 4, 5), thermomechanical control processing (Ref 6), and warm cross wedge rolling (Ref 7). Among them, ECAP is used most frequently, since it has the potential for scaling up to large samples and produces reasonably homogeneous microstructure without any reduction in the cross-sectional dimensions of the samples. Wang et al. (Ref 1) obtained the microduplex structures (ferrite + cementite) in a fully pearlitic 65Mn steel by ECAP via the C route (rotated by 180° along the longitudinal axis of the specimen after each pass) at 650 °C. In our previous study (Ref 8, 9), the Fe-0.8wt.%C steel with a full pearlitic structure was processed by ECAP via the Bc route (rotated clockwise by 90° along the longitudinal axis of the specimen after each pass) at 650 °C. The ECAP warm deformation promotes cementite spheroidization, and the ultrafine microduplex (ferrite + cementite) structure can be obtained. Also, toughness and ductility can be improved significantly with only small strength decrease. Wetscher et al. (Ref 10) deformed fully pearlitic R260 rail steel by ECAP at room temperature. The tensile strength increased with the number of ECAP passes. The fatigue crack growth rate and fracture toughness showed very strong azimuth anisotropy, closely related to the deformed cementite lamellae. However, most of the studies have focused on the lamellae pearlitic structure with high strength and high deformation resistance. Due to poor toughness and ductility, fracture can easily occur during the deformation process. However, the granular pearlite has poor strength and high toughness and ductility, which are beneficial for severe plastic deformation. To date, a few studies have reported ECAP of the granular pearlite steel. Thus, in this paper, the granular pearlite steel was processed by ECAP at room temperature. The underlying microstructure evolution mechanism was revealed and the mechanical properties were systematically studied. The results discussed in this paper can provide useful experimental support for the development and applications of the ultrafine-grained high carbon steels.

2. Materials and Experimental Procedure

The material used is commercial eutectoid steel with the following chemical composition (in wt.%): 0.82% C, 0.33% Mn, 0.24% Si, 0.011% P, 0.012% S, and Fe balance. After spheroidize annealing, the samples were treated at 1033 K for 2 h, and then cooled to 953 K for 8 h. When the temperature reduced to 773 K, the samples were removed from the furnace and air cooled. The samples used for ECAP were machined into cylindrical bars, 49 mm in length and 8.3 mm in diameter. The ECAP work was done at the Central Iron and Steel Research Institute for Structural Materials in Beijing, China. The detailed parameters of the mold and the ECAP process are listed in reference (Ref 9). The difference between this experiment and reference (Ref 9) is the extrusion temperature. The present processing was carried out at room temperature, while in reference (Ref 9) it was 923 K. After ECAP, the samples used for the metallographic investigation were cut from transverse

Yi Xiong and **Fengzhang Ren**, School of Materials Science and Engineering, Henan University of Science and Technology, Luoyang 471003, P.R. China and Collaborative Innovation Center of Nonferrous Metals, Luoyang 471003, P.R. China; **Tiantian He**, Institute of Metal Research, Chinese Academy of Sciences, Shenyang 110016, P.R. China; **Pengyan Li** and **Lufei Chen**, School of Materials Science and Engineering, Henan University of Science and Technology, Luoyang 471003, P.R. China; and **Alex A.Volinsky**, Department of Mechanical Engineering, University of South Florida, Tampa, FL 33620. Contact e-mails: xy_hbdy@163.com and tthe12b@imr.ac.cn.

cross sections by wire electrode cutting method, before and after ECAP, and then subjected to several successive steps of grinding and polishing. After that, the samples were etched in a 4 vol.% nitric acid solution. Scanning electron microscopy (SEM, Hitachi-S4300) was used for microstructure analysis. Transmission electron microscopy (TEM, JEM-2010) was used to examine the microstructure of the processed specimens. Thin foil mechanically polished down to 40 μm was utilized for TEM sample preparation using a double-jet electrolytic thinning technique (30 V, 50 mA) in a 93 vol.% acetic acid/7 vol.% perchloric acid mixture. Liquid nitrogen was used for cooling during the thinning process, with the temperature raising to no higher than 243 K. Uniaxial tensile tests were performed on the samples with the 2×0.5 mm^2 cross section and 10 mm gage length using an Instron 5848 Micro-Tester (2 kN) with 1×10^{-3} s^{-1} strain rate at room temperature. The tensile direction was parallel to the extrusion direction of the samples. The morphology of the fracture surfaces was observed using JSM-5610LV SEM. Microhardness was measured using MH-3 Vickers microhardness tester with 200 g normal load and 10 s holding time on the as-polished regions. Average microhardness values were determined based on five indentation measurements.

3. Results and Discussion

3.1 Microstructure Evolution Before and After ECAP

Figure 1 shows the SEM micrographs of granular pearlite steel before and after ECAP. It can be seen that after spheroidize annealing before ECAP, the cementite lamellae are almost completely spheroidized and the cementite particle size has non-homogeneous distribution. The size of the bulky cementite particles at the primary austenite grain boundary is about 1 μm, while the size of the cementite particles inside the primary austenite grain is about 500 nm. Some cementite lamellae can be observed in the form of a short bar, as seen in the outlined zone of Fig. 1(a). The average grain diameter of cementite particles is 750 nm. After one ECAP pass, due to the shear strain, the shape of some cementite lamellae changes from short bar to dumbbell, as indicated in Fig. 1(b) by the arrow. The large cementite particles are refined to a small size of ~500 nm. After two passes, in Fig. 1(c), the cementite particles are distributed along the deformation direction. The number of the large cementite particles decreased and the amount of small particles (~400 nm) increased. After four passes, in Fig. 1(d), most of the large cementite particles disappeared and many small particles (~250 nm) are distributed in the ferrite matrix. Under the severe plastic deformation of ECAP, the microstructure of granular pearlite is obviously different from the lamellar pearlite. In reference (Ref 8), the cementite lamella are bent, kinked, and fractured to coordinate the plastic deformation of the ferrite. At high temperature, the cementite spheroidization enhances with more ECAP passes. In the present work, the granular pearlite is mainly fragmented to coordinate the plastic deformation of the ferrite. With more ECAP passes, the cementite particles change from non-homogeneous distribution before ECAP to fine and homogeneous particles with the size of about 250 nm.

The TEM micrographs of the samples' microstructure before and after ECAP are shown in Fig. 2. After spheroidize annealing, most of the cementite lamellae are completely spheroidized, with only a few lamellae still present in the form of a short bar. The spheroidized cementite particle size has non-homogeneous distribution, which is consistent with Fig. 1(a). After one ECAP pass, a large number of dislocation lines are generated and accumulated in the elongated ferrite matrix, leading to the formation of high density tangled dislocations. The cementite particles as the secondary phase can effectively fix dislocations and inhibit their motion. After two passes, the dislocations arrange themselves into dislocation cells, and the dislocation cells become sharper, forming subgrains. Thus, the ferrite is refined with the grain size of about 500 nm. Meanwhile, the particle diameter of the cementite particles reduces to 300-500 nm. After four passes, the dislocation density decreases significantly, compared with the two passes. This is because, a large amount of dislocations are consumed when the subgrains transfer from the low-angle grain boundaries to the high-angle grain boundaries with strain accumulation (Ref 11, 12). Due to dynamic recovery, the ferrite has equiaxed shape with the grain size of about 400 nm, and the corresponding cementite particle diameter is about 200 nm. The corresponding grain refinement mechanism can be summarized as the following process: (1) development of dislocation lines in original grains; (2) the formation of dislocation tangles and dislocation cells due to the pile-up of dislocation lines; (3) accumulated strains become larger with the number of ECAP passes, transforming dislocation tangles and dislocation cells into subgrain boundaries; and (4) evolution of the continuous dynamic recovery subgrain boundaries into refined grain boundaries.

3.2 Mechanical Properties

The engineering stress-strain curves of the granular pearlite steel before and after different ECAP passes are shown in Fig. 3. It can be seen that the pearlite tensile strength increased, but the corresponding elongation reduced with more ECAP passes. The mechanical properties of granular pearlite before and after ECAP are listed in Table 1. The tensile and yield strength of the granular pearlite increased by 80 and 216%, from 598 and 289 MPa (before ECAP) to 1077 and 915 MPa (after four ECAP passes), respectively. The corresponding microhardness increased by 80% from 195 to 349 HV. The Vickers hardness is about 1/3 of the ultimate tensile strength value (Ref 13). Also, the ratio of the yield strength to tensile strength increased from 0.48 to 0.85, while the elongation reduced from 20.1 to 10.2%. After ECAP, large amounts of dislocation lines were generated and accumulated in the elongated ferrite matrix, leading to the formation of high density tangled dislocations, as seen in Figs. 2(b) and (c). The strength of the granular pearlite steel increased with more ECAP passes due to dislocation strengthening. Dynamic recovery occurred with the strain accumulation, and the ferrite grain was refined by the subgrain. After four passes, the ratio of yield strength to tensile strength of the ultrafine-grained steel reached 0.85, which is close to Li' result of 0.86, where the ultra-microduplex structure was produced in the eutectoid steel by warm deformation (Ref 14). This change in the ratio of yield strength to tensile strength can be attributed to different microstructure after different number of the ECAP passes. Similar changes in the mechanical strength due to hot deformation were reported in other studies of eutectoid steels, for example (Ref 15, 16). The granular pearlite steels transfer from dislocation strengthening (one ECAP pass) to grain refinement strengthening (four ECAP passes). Overall, granular

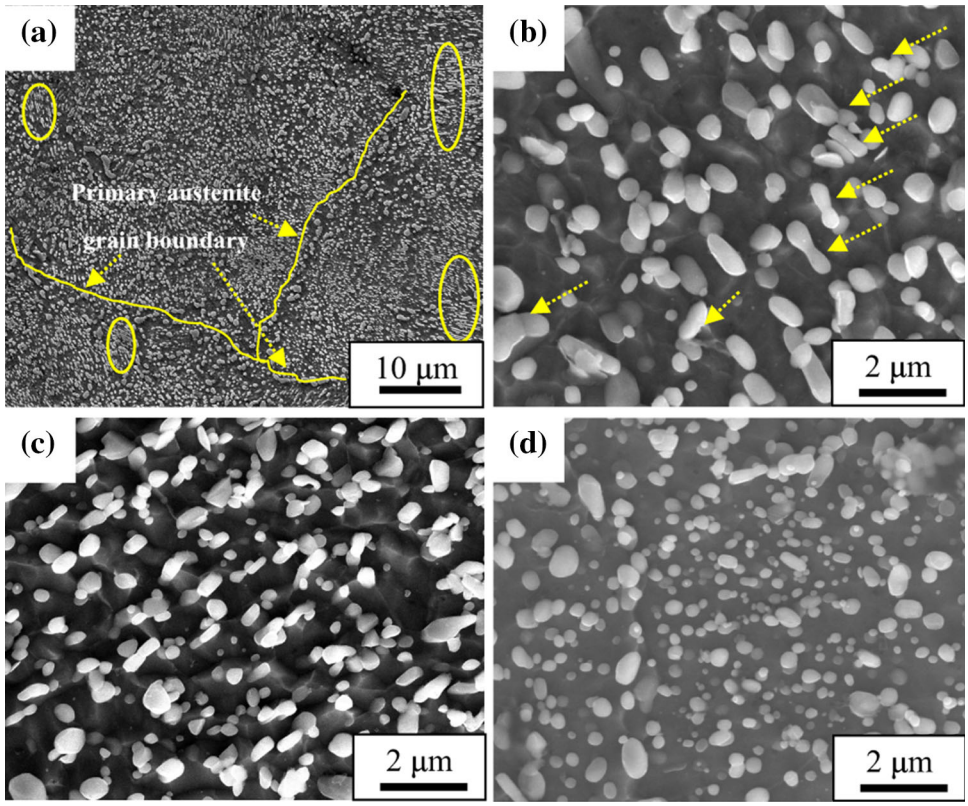

Fig. 1 SEM micrographs of the microstructure before and after different ECAP passes: (a) granular pearlite; (b) 1 pass; (c) 2 passes; and (d) 4 passes

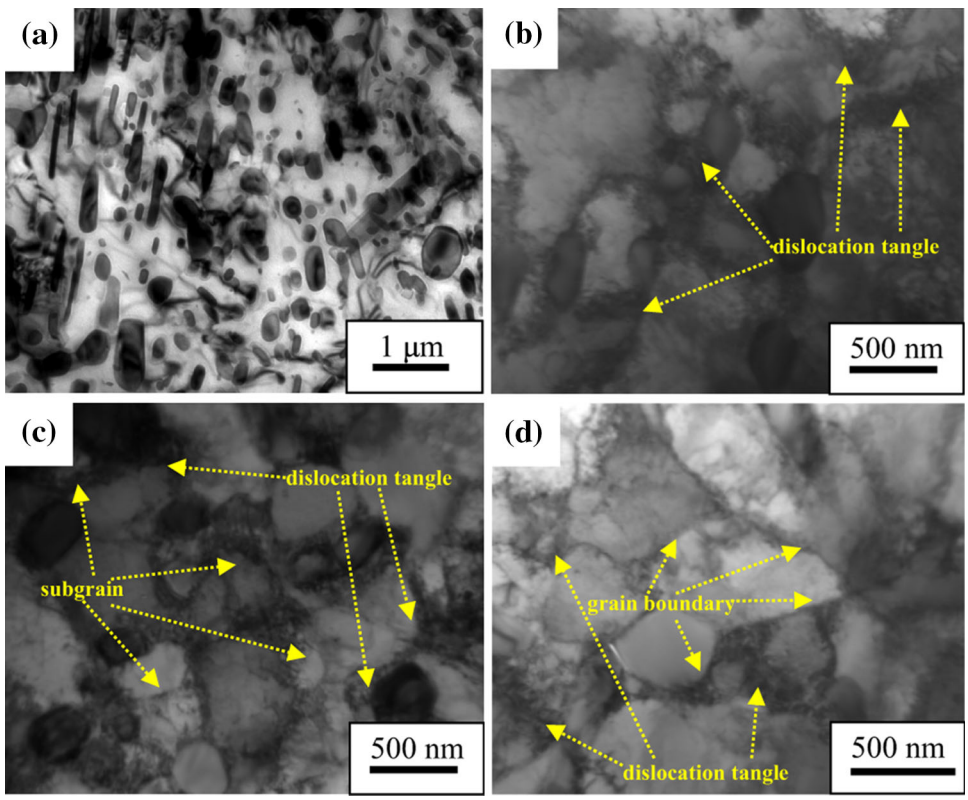

Fig. 2 TEM images of the microstructure before and after different ECAP passes: (a) granular pearlite; (b) 1 pass; (c) 2 passes; and (d) 4 passes

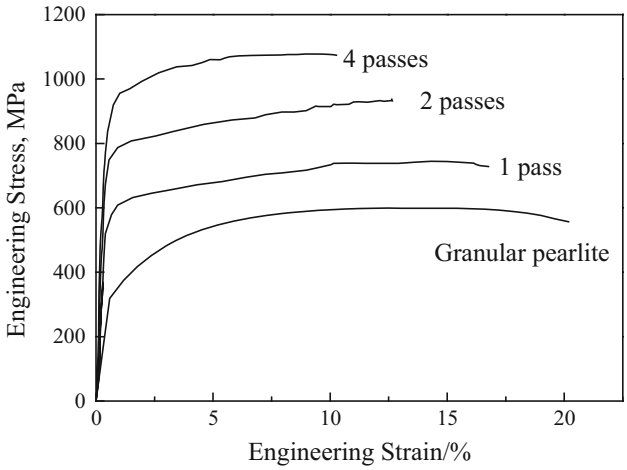

Fig. 3 Engineering stress-strain curves of the mini-tensile samples before and after ECAP

pearlite not only has high strength, but also some ductility after severe plastic deformation.

The fracture surface morphology of the granular pearlite before and after ECAP is shown in Fig. 4. Due to good plasticity, large and deep dimples along with lots of small and shallow ones can be found before ECAP. The dimples are distributed unevenly, with 10-30 μm large and deep ones and 2-5 μm small and shallow ones, as seen in Fig. 4(a). After a single ECAP pass, large and deep dimples disappear and large amounts of small and shallow ones with the average size of 3-5 μm are observed in Fig. 4(b). The dimples are unevenly distributed and a small amount of the quasi-cleavage-like fractures can be found in local areas. After two passes, the dimple size further reduced to 1-3 μm with more uniform distribution, compared with Fig. 4(a). A small amount of cleavage facets is present, indicating the increase of the quasi-cleavage-like fracture characteristics, as seen in Fig. 4(c), pointed by the arrow. With the ECAP passes increasing to four, the dimples are distributed more unevenly, compared with Figs. 4(b) and (c). The dimple depth reduces, while the number

Table 1 Mechanical properties and the cementite particle size of granular pearlite before and after ECAP

	Pearlite	1 pass	2 passes	4 passes
Hardness, HV	195	261	295	349
Yield strength ($\sigma_{s(0.2)}$), MPa	289	594	786	915
Tensile strength (σ_b), MPa	598	744	933	1077
$\sigma_{s(0.2)}/\sigma_b$	0.48	0.80	0.84	0.85
Elongation (δ), %	20.1	16.7	12.6	10.2
Cementite particle size, nm	750	500	400	250

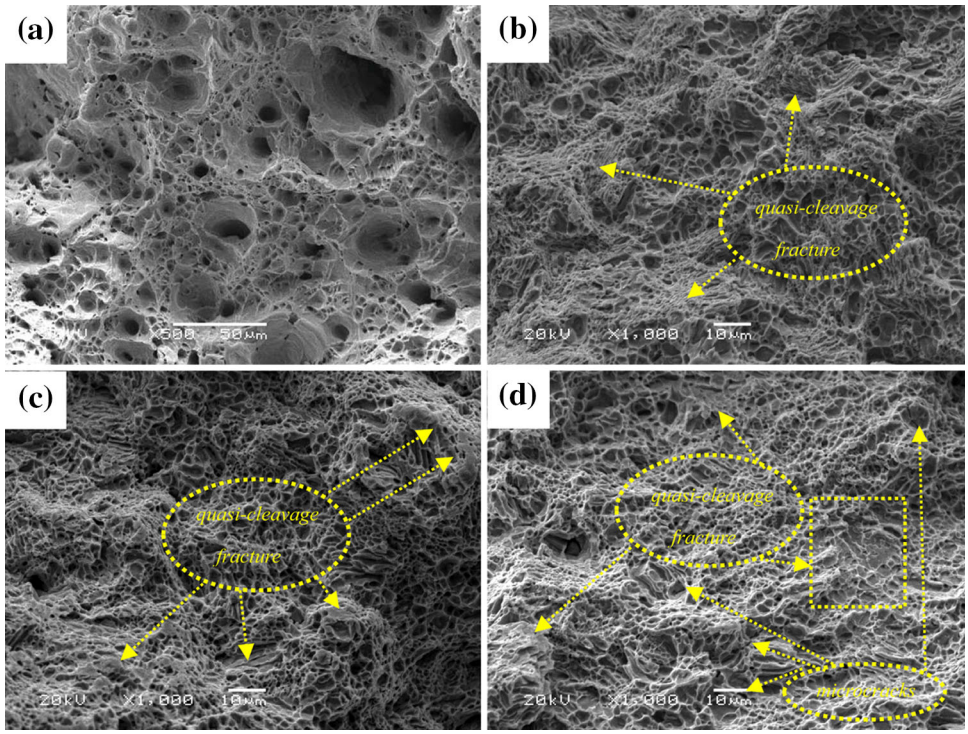

Fig. 4 Fracture surface morphology of the mini-tensile samples: (a) granular pearlite; (b) 1 pass; (c) 2 passes; and (d) 4 passes

of dimple increases and the dimple size decreases to 1 μm. The cleavage facets are expanded and some microcracks are present in local areas, pointed by the arrow in Fig. 4(d). However, the ferrite grain and the cementite particles refine to submicron with the number of ECAP passes, resulting in smaller dimple size and increased number of dimples. Meanwhile, few cementite lamellae with the shape of the short bar, which are not fully spheroidized, are arranged along the deformation direction. As a result, the fracture morphology of the granular pearlite changes from typical ductile fracture to ductile and quasi-cleavage fracture with the ECAP passes increasing. Similar phenomenon was observed in pure Cu after ECAP at room temperature by Ding et al. (Ref 17). The fracture morphology of pure Cu turned from ductile fracture to brittle fracture with the number of ECAP passes increasing, but the fracture mode was dominated by ductile fracture.

4. Conclusions

The granular pearlite high carbon steel was severely plastically deformed by ECAP up to four passes, at the room temperature, using the Bc route. The microstructure and mechanical properties were systematically characterized and analyzed. The results are as follows:

1. The ultra-microduplex structure with 400 nm equiaxed ferrite grains and 200 nm cementite particles was fabricated in the granular pearlite steel after four ECAP passes at room temperature via the Bc route. The ferrite grains were refined due to the continuous dynamic recovery.
2. The strength, microhardness, and the corresponding ratio of the yield to tensile strength increased with the number of ECAP passes. After four passes, the tensile strength, yield strength, microhardness, and the ratio of the yield to tensile strength increased to 1077, 915 MPa, 349 HV, and 0.85, respectively. Meanwhile, the elongation reduced from 20.1% (before ECAP) to 10.2% (after four ECAP passes).
3. With the ECAP passes increasing, the fracture morphology of the granular pearlite changed from typical ductile fracture to ductile and quasi-cleavage mixed fracture.

Acknowledgments

This work was supported by the National Natural Science Foundation of China under Grant No. 50801021 and 51201061, and by the program for the Young Key Teachers in the Henan Province under Grant No. 2011GGJS-070, and the Henan Province Program for Science and Technology Innovation Excellent Talents (144200510009).

References

1. J.T. Wang, J.X. Huang, Z.Z. De, Z. Zhang, X.C. Zhao, Microstructure Transformation in a Pearlite Steel During Equal Channel Angular Pressing. Ultrafine Grained Materials, 2004, p 673–678
2. Y. Ivanisenko, W. Lojkowski, R.Z. Valiev, and H.J. Fecht, The Mechanism of Formation of Nanostructure and Dissolution of Cementite in a Pearlitic Steel During High Pressure Torsion, *Acta Mater.*, 2003, **51**, p 5555–5570
3. C. Kammerhofer, A. Hohenwarter, S. Scheriau, H.P. Brantner, and R. Pippan, Influence of Morphology and Structural Size on the Fracture Behavior of a Nanostructured Pearlitic Steel, *Mater. Sci. Eng. A*, 2013, **585**, p 190–196
4. Z.G. Liu, X.J. Hao, K. Masuyama, K. Tsuchiya, M. Umemoto, and S.M. Hao, Nanocrystal Formation in a Ball Milled Eutectoid Steel, *Scripta Mater.*, 2001, **44**, p 1775–1779
5. Y. Xu, Z.G. Liu, M. Umemoto, and K. Tsuchiya, Formation and Annealing Behavior of Nanocrystalline Ferrite in Fe-0.89C Spheroidite Steel Produced by Ball Milling, *Metall. Mater. Trans. A*, 2002, **33**, p 2195–2203
6. T. Maki and T. Furuhara, Microstructure and Mechanical Property of Ultra-Fine (Ferrite + Cementite) Duplex Structure in High Carbon Steel, *Mater. Sci. Forum*, 2003, **426–432**, p 19–26
7. Y. Xiong, S.H. Sun, Y. Li, J. Zhao, Z.Q. Lv, D.L. Zhao, Y.Z. Zheng, and W.T. Fu, Effect of Warm Cross-Wedge Rolling on Microstructure and Mechanical Property of High Carbon Steel Rods, *Mater. Sci. Eng. A*, 2006, **431**, p 152–157
8. T.T. He, Y. Xiong, F.Z. Ren, Z.Q. Guo, and A.A. Volinsky, Microstructure of Ultra-Fine-Grained High Carbon Steel Prepared by Equal Channel Angular Pressing, *Mater. Sci. Eng. A*, 2012, **535**, p 306–310
9. Y. Xiong, T.T. He, Z.Q. Guo, H.Y. He, F.Z. Ren, and A.A. Volinsky, Mechanical Properties and Fracture Characteristics of High Carbon Steel After Equal Channel Angular Pressing, *Mater. Sci. Eng. A*, 2013, **563**, p 163–167
10. F. Wetscher, R. Stock, and R. Pippan, Changes in the Mechanical Properties of a Pearlitic Steel Due to Large Shear Deformation, *Mater. Sci. Eng. A*, 2007, **445–446**, p 237–243
11. A. Belyakov, T. Sakai, H. Miura, R. Kaibyshev, and K. Tsuzaki, Continuous Recrystallization in Austenitic Stainless Steel After Large Strain Deformation, *Acta Mater.*, 2002, **50**, p 1547–1557
12. J.Z. Lu, J.W. Zhong, K.Y. Luo, L. Zhang, F.Z. Dai, K.M. Chen, Q.W. Wang, J.S. Zhong, and Y.K. Zhang, Micro-structural Strengthening Mechanism of Multiple Laser Shock Processing Impacts on AISI, 8620 Steel, *Mater. Sci. Eng. A*, 2011, **528**, p 6128–6133
13. Compilations Group of "Mechanical properties of metals", Mechanical Properties of Metals, Mechanical Industry Press, Beijing, 1982, p. 230 (in Chinese)
14. C.S. Zheng, L.F. Li, W.Y. Yang, and Z.Q. Sun, Microstructure Evolution and Mechanical Properties of Eutectoid Steel with Ultrafine or Fine (Ferrite + Cementite) Structure, *Mater. Sci. Eng. A*, 2014, **599**, p 16–24
15. C.S. Zheng, L.F. Li, W.Y. Yang, and Z.Q. Sun, Enhancement of Mechanical Properties by Changing Microstructure in the Eutectoid Steel, *Mater. Sci. Eng. A*, 2012, **558**, p 158–161
16. L.F. Li, W.Y. Yang, and Z.Q. Sun, Microstructure Evolution of a Pearlitic Steel During Hot Deformation of Undercooled Austenite and Subsequent Annealing, *Metall. Mater. Trans. A*, 2008, **39**, p 624–635
17. Y.T. Ding, B. Liu, T.B. Guo, Y. Hu, H.L. Li, and J.Y. Zhao, Dislocation Density Variation and Mechanical Properties of Pure Copper Via Equal Channel Angular Pressing, *Chin. J. Nonferrous Met.*, 2014, **24**, p 2057–2064 ((in Chinese))